electronic reprint

CRYSTALLOGRAPHIC COMMUNICATIONS

ISSN: 2056-9890
journals.iucr.org/e

Diastereotopic groups in two new single-enantiomer structures (R_2)P(O)[NH-(+)CH(C_2H_5)(C_6H_5)] (R = OC_6H_5 and C_6H_5)

Farnaz Eslami, Mehrdad Pourayoubi, Fahimeh Sabbaghi, Eliška Skořepová, Michal Dušek and Sahar Baniyaghoob

Acta Cryst. (2023). E**79**, 769–776

Acta Cryst E CRYSTALLOGRAPHIC COMMUNICATIONS
ISSN 2056-9890

Diastereotopic groups in two new single-enantiomer structures $(R_2)P(O)[NH\text{-}(+)CH(C_2H_5)\text{-}(C_6H_5)]$ (R = OC_6H_5 and C_6H_5)

Farnaz Eslami,[a] Mehrdad Pourayoubi,[b]* Fahimeh Sabbaghi,[c] Eliška Skořepová,[d] Michal Dušek[d] and Sahar Baniyaghoob[a]

[a]Department of Chemistry, Science and Research Branch, Islamic Azad University, Tehran, Iran, [b]Department of Chemistry, Faculty of Science, Ferdowsi University of Mashhad, Mashhad, Iran, [c]Department of Chemistry, Zanjan Branch, Islamic Azad University, Zanjan, Iran, and [d]Institute of Physics of the Czech Academy of Sciences, Na Slovance 2, 182 21, Prague 8, Czech Republic. *Correspondence e-mail: pourayoubi@um.ac.ir

Received 17 March 2023
Accepted 19 July 2023

Edited by V. Jancik, Universidad Nacional Autónoma de México, México

Keywords: phosphoramide; phosphinamide; single-enantiomer; diastereotopic groups; X-ray crystallography; crystal structure.

Supporting information: this article has supporting information at journals.iucr.org/e

The crystal structures of two single-enantiomer compounds, *i.e.* diphenyl [(*R*)-(+)-α-ethylbenzylamido]phosphate, $C_{21}H_{22}NO_3P$ or $(C_6H_5O)_2P(O)[NH\text{-}(R)\text{-}(+)CH(C_2H_5)(C_6H_5)]$ (**I**), and *N*-[(*R*)-(+)-α-ethylbenzyl]-*P*,*P*-diphenylphosphinic amide, $C_{21}H_{22}NOP$ or $(C_6H_5)_2P(O)[NH\text{-}R\text{-}(+)CH(C_2H_5)(C_6H_5)]$ (**II**), were studied. The different environments at the phosphorus atoms, $(O)_2P(O)(N)$ and $(C)_2P(O)(N)$, allow the P═O/P—N bond strengths to be compared, as well as the N—H···O═P hydrogen-bond strengths, and P═O/N—H vibrations. The following characteristics related to diastereotopic C_6H_5O/C_6H_5 groups in **I**/**II** were considered: geometry parameters, contributions to the crystal packing, solution $^{13}C/^{1}H$ NMR chemical shifts, conformations, and NMR coupling constants. The phosphorus-carbon coupling constants $^{n}J_{PC}$ (n = 2 and 3) in **I** and $^{m}J_{PC}$ (m = 1, 2, 3 and 4) in **II** were evaluated. For a comparative study, chiral analogous structures were retrieved from the Cambridge Structural Database (CSD) and their geometries and conformations are discussed.

1. Chemical context

Phosphoramide/phosphinamide moieties are well-known structural motifs of some bioactive products and drugs (Warren *et al.*, 2016; Palacios *et al.*, 2005). There are also reports on their applications in flame retardants (Nguyen & Kim, 2008), ligands (Wang *et al.*, 2021; Ferentinos *et al.*, 2019; Zhang *et al.*, 2019), extractants (Akbari *et al.*, 2019), anion transporters (Cranwell *et al.*, 2013) and catalysts (Klare *et al.*, 2014).

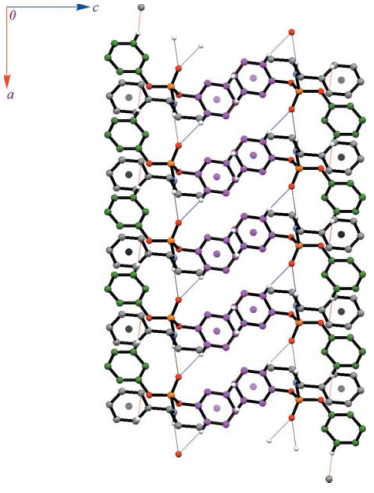

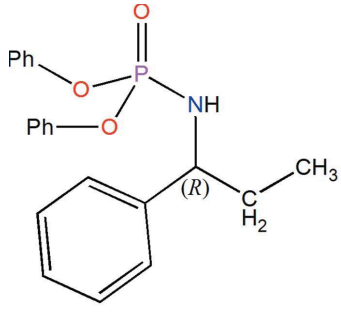

I

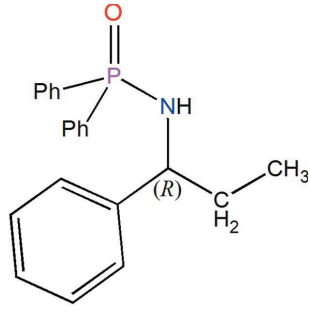

II

Some of these characteristics are general for phosphoramide/phosphinamide compounds, and can be influenced by the groups attached to the common NP═O unit. Typically, the

donor property of the phosphoryl group is beneficial in sorption processes, interactions with some enzymes and the formation of hydrogen bonds (Corbridge, 2000). The subfamily to which the compounds belong also plays a role. For example, phosphinicamides with the $(C)_2P(O)(N)$ skeleton are found to have higher electron-donor properties with respect to amidophosphodiesters with the $(O)_2P(O)(N)$ skeleton. The chirality may also be essential for some particular applications, such as the manufacture of drugs and the planning of some reactions related to different reactivities of diastereotopic groups (Nakayama & Thompson, 1990), enantioseparation (Ahmadabad *et al.*, 2019) and enantioselective catalysis (Liao *et al.*, 2019).

Recently, we have reported some single-enantiomer small molecules, belonging to the phosphoramide family, and phosphoramide-based macromolecules/hydrogels (Ahmadabad *et al.*, 2019; Taherzadeh *et al.*, 2021; Sabbaghi *et al.*, 2019). The related synthesis procedure could also be developed for manufacturing phosphinamide-based materials. Moreover, we are interested in studying the differences between two diastereotopic groups in chiral structures. The reason for such attention is the asymmetric induction at phosphorus by the chiral group, which causes different reactivities of two diastereotopic groups (Nakayama & Thompson, 1990). These differences were investigated in organic syntheses for the creation of new stereocentres and also can be used for the design and synthesis of ligands with different donor properties of the diastereotopic groups.

In the present work, we continue with the synthesis of new chiral $(C_6H_5O)_2P(O)[NH\text{-}(+)CH(C_2H_5)(C_6H_5)]$ phosphoramide, (**I**), and $(C_6H_5)_2P(O)[NH\text{-}(+)CH(C_2H_5)(C_6H_5)]$ phosphinamide, (**II**) to study structural differences of two diastereotopic C_6H_5O/C_6H_5 groups, caused by the same chiral amine. Structure **I** is the enantiomer of the previously reported $(C_6H_5O)_2P(O)[NH\text{-}(-)CH(C_2H_5)(C_6H_5)]$ (Sabbaghi *et al.*, 2011). The investigation is completed by considering structural differences/similarities of diastereotopic groups in analogous chiral structures retrieved from the CSD (Groom *et al.*, 2016). The main features of the NMR parameters of the diastereotopic groups in **I** and **II** are also discussed.

2. Structural commentary

Compound **I** crystallizes in the orthorhombic chiral space group $P2_12_12_1$, with the asymmetric unit composed of one amidophosphodiester molecule (Fig. 1). Compound **II** is triclinic in chiral space group $P1$, and its asymmetric unit consists of two phosphinicamide molecules (Fig. 2). Selected bond lengths and angles are presented in Tables 1 and 2. All bond distances and angles are within the values observed in analogous structures (Vahdani Alviri *et al.*, 2020; Hamzehee *et al.*, 2017).

The P atoms display a distorted tetrahedral environment, $(O)_2P(O)(N)$ for **I** and $(C)_2P(O)(N)$ for **II**, and the maximum/minimum bond angles at phosphorus are related to O═P—O/O—P—O and O═P—N/N—P—C. The differences between maximum and minimum values are about 16.8° for **I** and 17.5°/16.9° for the two symmetry-independent molecules of **II**. The P—N—C angles in **I** and **II**, for example, P1—N3—C4 angle in **II** of 120.91 (14)° (Table 2), demonstrate that the hybridization state of nitrogen atoms is close to sp^2. The P—O—C angles of **I**, 127.68 (17)°/121.91 (16)°, similarly show the hybridization state of the ester oxygen atoms is close to sp^2.

The structure **I** is similar to its *S*-enantiomer (EXIQIM; Sabbaghi *et al.*, 2011) regarding space group, unit cell and other structural parameters; the only substantial difference is related to the configuration at dissymmetric carbon atoms. Fig. 3*a* shows the overlay of the inverted structure of **I** with

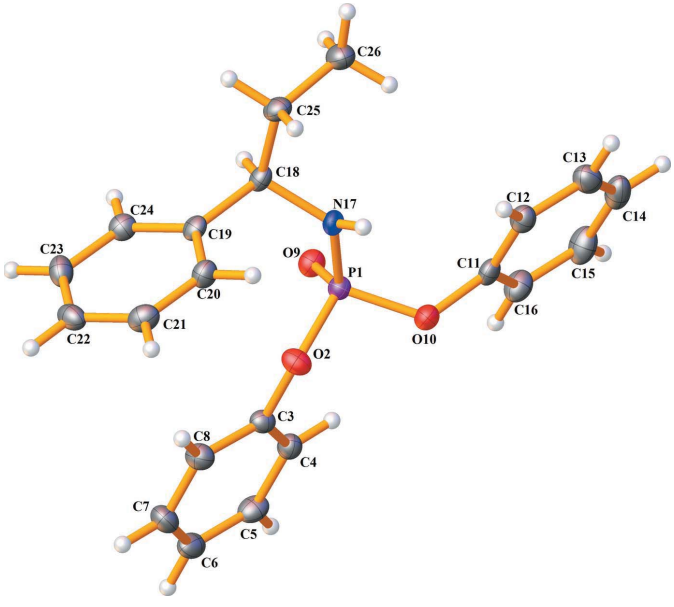

Figure 1
The asymmetric unit of **I**, showing the atom-numbering scheme for non-hydrogen atoms and displacement ellipsoids at 50% probability level. Hydrogen atoms are drawn as spheres of arbitrary radii.

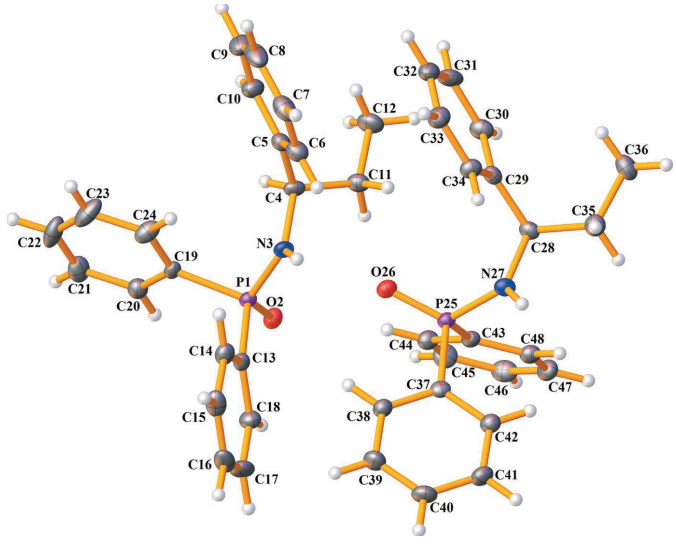

Figure 2
Displacement ellipsoid plot (50% probability) of the asymmetric unit of **II**, showing the atom-numbering scheme for non-hydrogen atoms. Hydrogen atoms are drawn as spheres of arbitrary radii.

Table 1
Selected geometric parameters (Å, °) for **I**.

P1—O2	1.5814 (18)	O2—C3	1.390 (3)
P1—O9	1.469 (2)	O10—C11	1.411 (3)
P1—O10	1.5924 (19)	N17—C18	1.482 (3)
P1—N17	1.619 (2)		
O2—P1—O9	113.77 (11)	O2—C3—C8	114.9 (2)
O2—P1—O10	99.62 (10)	P1—O10—C11	121.91 (16)
O9—P1—O10	116.45 (11)	O10—C11—C12	119.5 (2)
O2—P1—N17	106.00 (11)	O10—C11—C16	118.5 (3)
O9—P1—N17	114.90 (12)	P1—N17—C18	120.34 (18)
O10—P1—N17	104.43 (11)	N17—C18—C19	112.8 (2)
P1—O2—C3	127.68 (17)	N17—C18—C25	108.4 (2)
O2—C3—C4	123.5 (2)		

EXIQIM. The overlay is calculated with a root-mean-square deviation (r.m.s.d.) of 0.0089 Å and a maximum deviation of 0.0153 Å.

The P═O bond in **I**, 1.469 (2) Å, is shorter than the P═O bonds in **II**, 1.4846 (15)/1.4933 (15) Å, and the same is true about the P—N bonds [1.619 (2) Å in **I**, and 1.6367 (19)/1.6426 (19) Å in **II**]. The differences result from the effect of electronegative oxygen atoms of two C_6H_5O groups in **I** attached to phosphorus, while in **II**, there are two C_6H_5 groups. The longer P—N bond in **II** is also caused by the steric effects of two phenyl groups directly attached to phosphorus. Minor differences are observed for the bond lengths related to the diastereotopic pairs. Typically, the P—O and P—C bonds in **I** and two independent molecules of **II** are 1.581 (2)/1.592 (2) Å, 1.802 (2)/1.808 (2) Å and 1.808 (2)/1.797 (2) Å.

In compound **I**, the N—H unit adopts an antiperiplanar (*–ap*) orientation with respect to the P═O group (based on the O═P—N—H torsion angle of −157.18°), and in two symmetry-independent molecules of **II**, the same units adopt synclinal (*–sc* and *+sc*) conformations (the torsion angles are −80.63° and +84.78°). The different conformation of **II** (in comparison to **I**) results from intramolecular rotations of the chiral amine, and the two independent molecules feature different rotations, but with a similar O═P—N—H conformation.

In **II**, the symmetry-independent molecules are similar concerning the bond lengths and angles (see Table 2). However, they show some differences in torsion angles (and

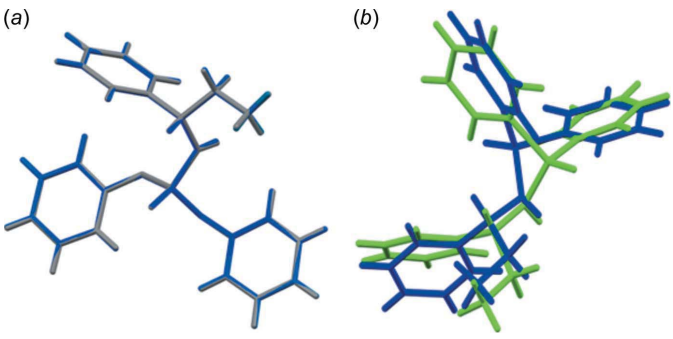

Figure 3
(*a*) Overlay of EXIQIM (grey) and inverted **I** (blue). (*b*) Overlay of two symmetry-independent molecules of **II** (green and blue show molecules P1 and P25, respectively).

Table 2
Selected geometric parameters (Å, °) for **II**.

P1—O2	1.4846 (15)	P25—O26	1.4933 (15)
P1—N3	1.6367 (19)	P25—N27	1.6426 (19)
P1—C13	1.802 (2)	P25—C37	1.808 (2)
P1—C19	1.808 (2)	P25—C43	1.797 (2)
N3—C4	1.474 (2)	N27—C28	1.469 (3)
O2—P1—N3	119.94 (9)	O26—P25—N27	119.61 (9)
O2—P1—C13	111.80 (9)	O26—P25—C37	109.99 (9)
N3—P1—C13	102.43 (10)	N27—P25—C37	102.69 (10)
O2—P1—C19	110.23 (9)	O26—P25—C43	110.87 (9)
N3—P1—C19	105.15 (10)	N27—P25—C43	104.84 (10)
C13—P1—C19	106.21 (9)	C37—P25—C43	108.07 (10)
P1—N3—C4	120.91 (14)	P25—N27—C28	122.16 (15)
N3—C4—C5	110.46 (17)	N27—C28—C29	114.02 (17)
N3—C4—C11	110.64 (17)	N27—C28—C35	107.53 (17)
P1—C13—C14	121.84 (17)	P25—C37—C38	117.22 (16)
P1—C13—C18	118.28 (17)	P25—C37—C42	123.28 (17)
P1—C19—C20	119.48 (17)	P25—C43—C44	118.93 (17)
P1—C19—C24	121.36 (18)	P25—C43—C48	122.26 (18)

conformations). Typically, the conformations in the CH_3—CH_2—CH—NH—P═O segment are defined by the C—C—C—N/C—C—N—P/C—N—P═O torsion angles, and the values in the P1 molecule of +173.7 (2)°/−98.2 (2)°/60.7 (2)° correspond to *+ap*/*−ac*/*+sc* conformations (*ac* = anticlinal). Similar torsion angles in the other molecule, −178.3 (2)°/−158.6 (2)°/−62.0 (2)°, define *−ap*/*–ap*/*−sc* conformations. The other notable difference between the two molecules is reflected in the direction of the phenyl ring of the chiral segment with respect to the P═O group (an opposite direction in the molecule P1 and the same direction in the second molecule). Fig. 3*b* shows the overlay of two molecules, and the root-mean-square deviation (r.m.s.d.) of the fit of them is 1.3533 Å with a maximum deviation of 4.6684 Å. The noted difference is reflected in the spatial distances of phenyl groups bonded to P and the phenyl group of chiral amine in the two molecules. The differences in diastereotopic phenyl rings in each molecule can also be described by their distances from the phenyl ring of the chiral amine.

For **I**, the distances between the centroid of the phenyl ring of chiral amine and the centroids of two diastereotopic phenyl groups are 5.0848 (1) and 7.9514 (1) Å. For the two symmetry-independent molecules of **II**, equivalent distances are 5.5767 (5)/7.0325 (6) Å and 7.1614 (6)/6.4951 (3) Å. These spatial distances show that one of the diastereotopic phenyl rings is significantly closer to the phenyl of the chiral amine. The differences in these spatial distances are pronounced in **I**, where the flexibility is greater (because of the existence of the P—O—C segment and the possibility of rotation).

In **I**, the conformations of phenyl rings can be introduced by the C—C—O—P torsion angles, which are 32.1 (3)°/−149.9 (2)° and 86.7 (3)°/−98.0 (3)° according to the *+sc*—*ac* conformations for both phenyl rings. In the structure of **II**, the C—C—P═O torsion angles were considered for checking the conformations of the phenyl rings. The values are 173.8 (2)°/−10.4 (2)° and 25.4 (2)°/−158.0 (2)° (*+ap*—*sp* and *+sp*—*ap*) in one molecule and 10.8 (2)°/−169.6 (2)° and −18.4 (2)°/163.0 (2)° (*+sp*—*ap* and *−sp*+*ap*) in the other molecule, which also show similar conformations.

Table 3
Hydrogen-bond geometry (Å, °) for **I**.

D—H···A	D—H	H···A	D···A	D—H···A
C12—H121···O9^{i}	0.94	2.55	3.474 (4)	170
N17—H171···O9^{i}	0.85	2.24	3.074 (4)	166 (2)

Symmetry code: (i) $x+1, y, z$.

Table 4
Hydrogen-bond geometry (Å, °) for **II**.

D—H···A	D—H	H···A	D···A	D—H···A
N27—H271···O2^{i}	0.84	2.08	2.923 (4)	176 (2)
N3—H31···O26	0.86	1.97	2.817 (4)	173 (2)

Symmetry code: (i) $x-1, y, z$.

3. Supramolecular features

In the crystal structures of **I** and **II**, the molecules are assembled in a chain arrangement through N—H···O(P) hydrogen bonds along [100] (Fig. 4, Tables 3 and 4). The N—H···O(P) hydrogen bond in **I** is weaker than in **II** (H···O distances are 2.24 and 1.97/2.08 Å, respectively). This weakness is the result of the lower hydrogen-bond acceptor capability expected for the phosphoryl group of an $(O)_2(N)P(O)$-based structure, compared to the phosphoryl group of a $(C)_2(N)P(O)$-based structure, and is due to the two atoms with a higher electronegativity bonded to the phosphorus atom. The effect of different electronegativities was previously noted (*see above*) for different P═O bond lengths.

C—H···π interactions in **I** assemble the molecules in a two-dimensional array in the *ab* plane. Fig. 5 shows the molecular assembly formed by the N—H···O, C—H···O and possible C—H···π interactions, where the C—H···O interaction does not change the dimensionality made by the N—H···O hydrogen bond. To show better the contact(s) contributing by each phenyl ring, the rings are distinguished by colours: green (C3–C8) and magenta (C11–C16) for the diastereotopic rings and grey (C19–C24) for the phenyl ring of the chiral amine. The green ring takes part in a C—H···π interaction as a donor (the acceptor is the grey ring) (H···Cg = 2.81 Å). The magenta ring takes part in a C—H···π interaction with an adjacent

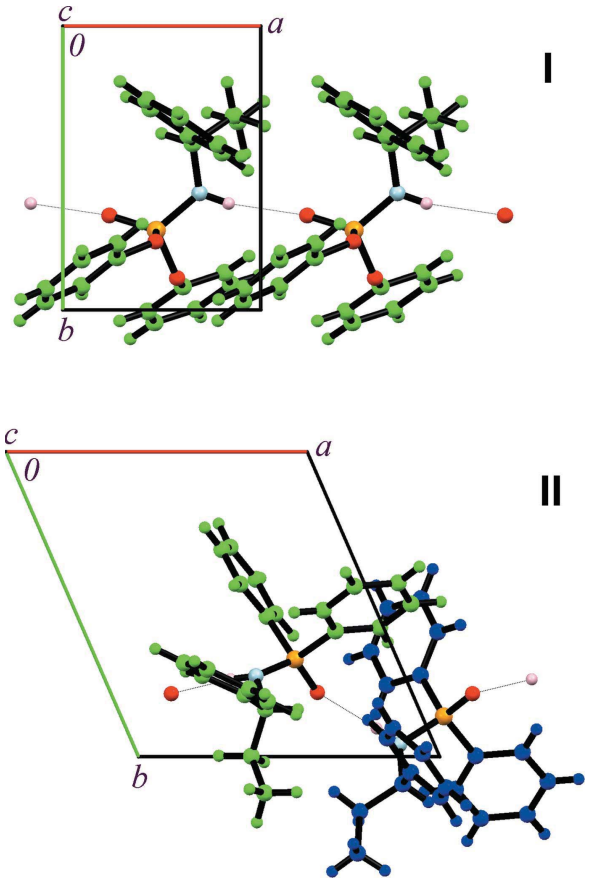

Figure 4
Crystal packing of **I** (top) and **II** (bottom). The red, orange, light-blue and pink balls show oxygen, phosphorus, nitrogen and hydrogen attached to nitrogen atoms. For **I**, carbon atoms and attached hydrogen atoms are shown in light green. For **II**, two-symmetry independent molecules are shown in light green and blue. The dotted lines show N—H···O hydrogen bonds.

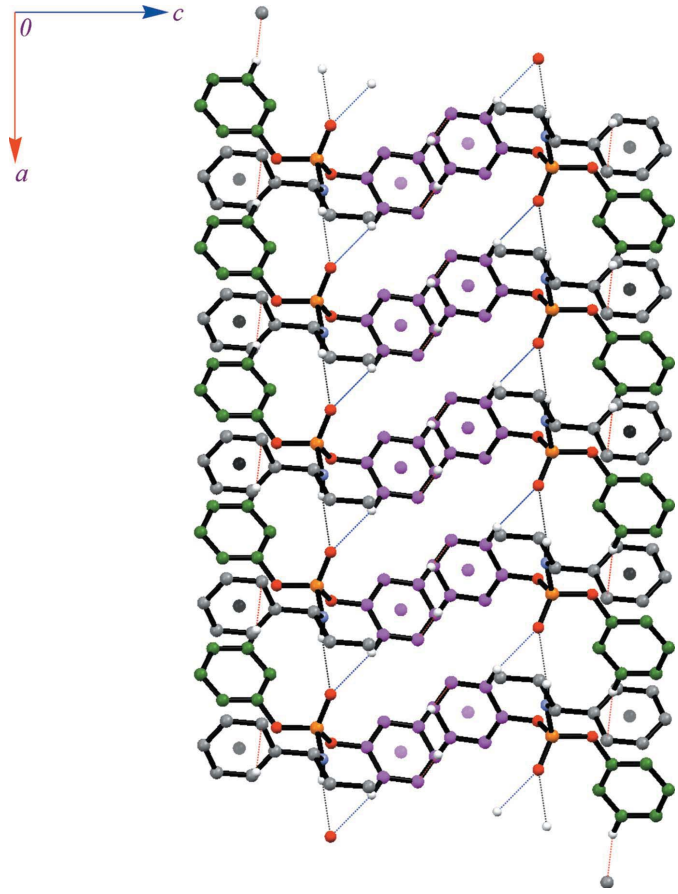

Figure 5
A view of the two-dimensional double-layered arrangement of **I** formed by N—H···O, C—H···O and C—H···π interactions (shown as black, blue and red dotted lines, respectively). The centroids of the phenyl rings taking part as acceptors in C—H···π interactions are shown as balls of the same colours as the corresponding ring.

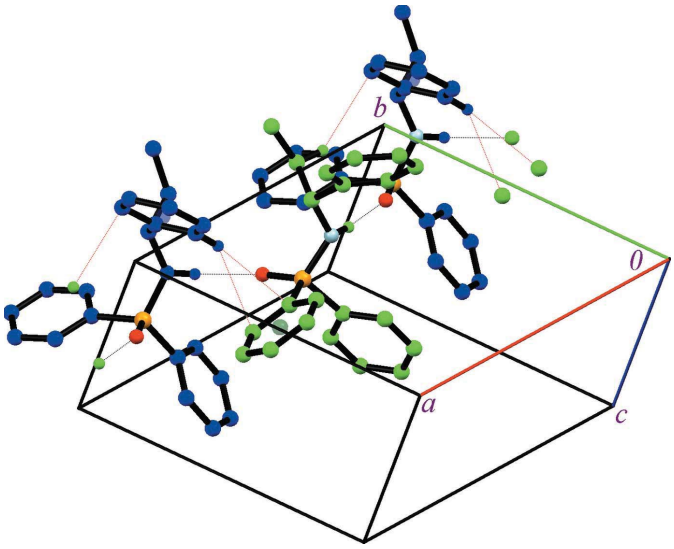

Figure 6
A view of the one-dimensional arrangement of structure **II** formed by N—H···O and C—H···π interactions (shown as black and red dotted lines). Only the hydrogen atoms participating in these hydrogen-bond interactions are shown.

symmetry-related magenta ring (H···*Cg* = 3.23 Å) and also in a C—H···OP interaction (H···O = 2.55 Å). The formed two-dimensional assembly is double-layered and has a thickness of 18.057 Å in the *c*-axis direction.

In the structure of **II**, two possible C—H···π interactions exist (H···*Cg* distances of 3.41 and 3.49 Å), which do not change the dimensionality made by the N—H···O hydrogen bonds. In both C—H···π interactions, the H donors are chiral amines of two symmetry-independent molecules (the *ortho*-hydrogen atom and the hydrogen of the CH_2 unit, as shown in Fig. 6). The acceptors are one of the diastereotopic phenyl rings of the molecule including atom P1 and the phenyl ring of the chiral amine in the other molecule.

4. An overview of diastereotopic groups in analogous structures

The chiral structures with an $R_2P(=X)$—N—C(H)(**C**)(C—C) fragment (*X* = O, S, N; **C** is a dissymmetric carbon atom) were retrieved from the CSD to study possible structural differences for diastereotopic *R* groups; the metal complexes were not considered. The CSD (version 5.42 updated on Feb. 2021; Groom *et al.*, 2016) comprises 48 such structures, of which two were unavailable. The remaining 46 structures include 79 pairs of diastereotopic P—*Y* (*Y* = C, O, N) bonds, and the structures have different skeletons, $(C)_2P(O)(N)$, $(C)_2P(S)(N)$, $(C)_2P(N)(N)$, $(O)_2P(O)(N)$ and $(N)_2P(O)(N)$. The related bond lengths are given in Table S1 of the supporting information. The largest difference for the P—C bond lengths made by diastereotopic groups (0.025 Å) exceeds the largest differences for the P—O (0.017 Å) and P—N bond lengths (0.015 Å). The P—C, P—N and P—O bond lengths in these structures vary from 1.773 to 1.837 Å, 1.629 to 1.652 Å and 1.555 to 1.607 Å, respectively, with averages of 1.805, 1.643 and 1.580 Å.

The conformations of diastereotopic groups attached to phosphorus were analysed in the structures analogous to **I** and **II**, *i.e.* with the O_2P and C_2P skeletons. Only three O_2P-based structures (with the oxygen atom attached to an arene ring) were found in the CSD. For the C_2P skeleton, 36 structures, including 64 R_2PX fragments, were checked, and the C—C—P═*X* (*X* = O, N, S) torsion angles were evaluated.

The C_2P-based structures mainly include $Ph_2P(O)$ fragment (28 structures), similar to compound **II**; however, structures with $Ph_2P(S)$ (seven structures), and $(C_6H_{11})_2P(=N)$ (one structure) fragments were also found. Both similar and different conformations were observed for diastereotopic groups. Details of the analysis are given in Table S2 and Fig. S1 of the supporting information. The torsion angles such as C—C—P═O of 0.04° in the structure with refcode MEFCIK (Sweeney *et al.*, 2006) show the P═O group nearly in a plane where the phenyl ring also exists. Its complementary torsion angle for the other C—C—P═O related to this phenyl ring is 176.54°, and these two torsion angles define the *sp*+*ap* conformation of this phenyl ring with respect to the P═O group. On the other hand, most of the structures also include ±*sp*±*ap* conformations at least for one phenyl ring. The most populated conformations for diastereotopic fragments (separated by "/") are ±*sp*±*ap*/±*sp*±*ap* (26 entries) and ±*sp*±*ap*/±*sc*±*ac* (23 entries). In the systems with phenyl rings directly attached to the phosphorus atom, as a result of crowding, the simultaneous torsion angles around ±90° (a perpendicular conformation) for both phenyl rings were not found for any structure. In some cases, like in the structure with refcode VUGSOG (Yin *et al.*, 2009) with close phenyl rings, the CH unit of one phenyl ring is directed toward the centroid of the second phenyl ring because of the formation of an intramolecular C—H···π interaction.

As a result of the existence of C—O—P moiety in the O_2P-based structures, the flexibility is expected to be higher than for Ph_2P-based structures; the three structures show different conformations but they include ±*sc*±*ac* conformations at least in one arene ring.

5. Hirshfeld surface analyses and fingerprint plots of structures I and II

To visualize and compare the intermolecular contacts of **I** and **II**, the Hirshfeld surfaces (HS) mapped with d_{norm} and two-dimensional fingerprint plots (Spackman & Jayatilaka, 2009; Spackman *et al.*, 2021) were generated using the *CrystalExplorer* program (Wolff *et al.*, 2013). In the HS map of **I** (Fig. 7), the red areas are associated with the N—H···O, C—H···O and 2×C—H···π interactions [labels (i), (ii) and (iii)]. The contacts of **I**, obtained from the fingerprint plots, are H···H (57.3%), H···C (28.8%), H···O (12.7%) and O···C (1.2%). The O···C contact results from the near distance of two symmetry-related phenoxy groups [O2(C3–C8)], through the ester oxygen atom and π-system.

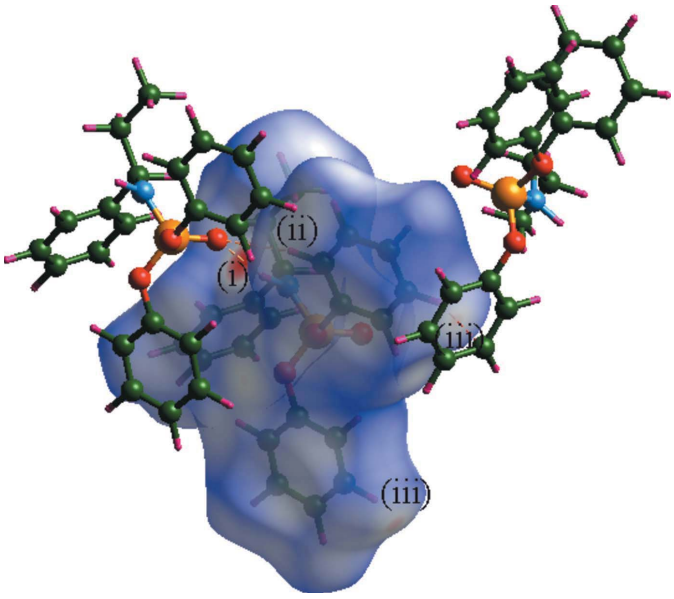

Figure 7
Hirshfeld surface map generated for the structure **I**. Two molecules are shown outside the surface to represent the N—H···O [label (i)], C—H···O [label (ii)] and typical C—H···π [label (iii)] interactions with the molecule within the surface.

For **II**, the HS map was generated around two symmetry-independent molecules step by step. Besides N—H···O hydrogen bonds, a significant H···H contact develops a red area, as seen in Fig. 8. This interaction is between H231 of the phenyl ring of molecule P1 connected to H301 of the chiral amine of the other molecule. The H···H separation was obtained as 2.291 Å and 2.026 Å in the X-ray and Hirshfeld analyses, respectively (the neutron-normalized CH distance is 1.083 Å in Hirshfeld in comparison with 0.941/0.943 Å in X-ray).

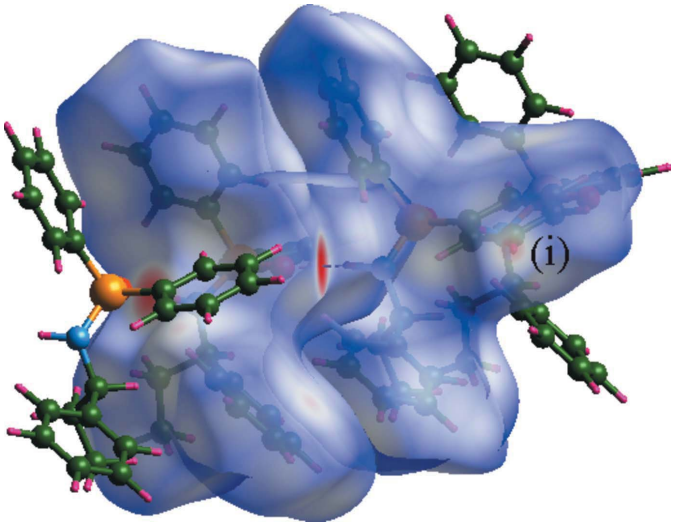

Figure 8
Hirshfeld surface map generated step by step around two symmetry-independent molecules of **II**. The two molecules outside the surface were given to show the hydrogen-bond interactions with the molecules within the surface. The red region labelled (i) is related to a close H···H contact between the molecules within and outside the surface (not shown).

The contribution percentages of various contacts were obtained for the two symmetry-independent molecules. Compared with **I**, the structure of **II** shows fewer H···O, H···C and O···C contacts (7.1%/7.0%, 26.1%/25.6%, 0.1% for both), which were compensated with remarkable H···H (64.2%/64.8%), and C···C contacts (2.5% for both). The smaller volume/Z ratio in **II** is reflected by the crowding, manifested in increased H···H contacts and the observation of C···C contacts.

6. Spectroscopy of I and II

In the IR spectra, the N—H stretching bands are centred at 3268 cm^{-1} for **I** and 3152 cm^{-1} for **II**. The lower NH stretching wave number of **II** is attributed to stronger N—H···OP hydrogen bonds as discussed in the X-ray crystallography section. The bands at 1244 cm^{-1} for **I** and 1192 cm^{-1} for **II** are assigned to the P═O vibrations, and the higher wave number for **I** is in accordance with the presence of more electronegative atoms in the $(O)_2P(O)N$ skeleton [*versus* $(C)_2P(O)N$ for **II**].

In the ^{13}C NMR spectra, the doublet signals at 31.80 p.p.m. (^3J = 8.1 Hz) for **I** and at 32.62 p.p.m. (^3J = 4.7 Hz) for **II** correspond to the CH_2 group. The dissymmetric carbon atom does not show coupling with phosphorus, and the *ipso*-C atom attached to it, *i.e.* with a three-bond separation from phosphorus, shows a doublet at 143.04 p.p.m. (^3J = 3.0 Hz) in **I** and at 145.50 p.p.m. (^3J = 4.6 Hz) in **II**.

For the two diastereotopic C_6H_5O groups in **I**, two sets of carbon signals are observed. For example, the doublets at 150.74/150.92 p.p.m. and 120.12/120.23 p.p.m., with ^2J = 7.0 Hz for the first pair and ^3J = 4.0 Hz for the second pair, are associated with the diastereotopic *ipso*-C atoms and diastereotopic *ortho*-C atoms, respectively. All carbon atoms of diastereotopic phenyl groups in compound **II** show couplings with phosphorus (^1J, ^2J, ^3J and ^4J).

The doublet signals at 131.74/131.86 p.p.m. (J = 1.9/2.1 Hz) are assigned to the *para*-carbon atoms of the phenyl rings with four bonds separation from the phosphorus atom. The doublets at 132.20/132.38 p.p.m. (J = 9.4/9.5 Hz) and at 128.62/128.82 p.p.m. (J = 12.2/12.1 Hz) are assigned to the diastereotopic *ortho*- and *meta*-carbon atoms. The doublets centred at 134.44 and 134.77 p.p.m. (J = 127.4 and 126.4 Hz) are related to the diastereotopic *ipso*-carbon atoms. The separation of these signals is comparable with previously investigated ^1J coupling constants for analogous compounds, typically in $(C_6H_5)_2P(O)$(NH-*cyclo*-C_7H_{13}) with ^1J = 129.4 Hz (Hamzehee *et al.*, 2017).

A brief discussion of ^{31}P NMR and ^1H NMR spectroscopy is given in the supporting information (Figures S2 to S11).

7. Conclusions

The differences/similarities of diastereotopic pairs, 2×C_6H_5O/2×C_6H_5, were discussed for two new single-enantiomer structures, $(C_6H_5O)_2P(O)$[NH-(+)CH$(C_2H_5)(C_6H_5)$] (**I**), and $(C_6H_5)_2P(O)$[NH-(+)CH$(C_2H_5)(C_6H_5)$] (**II**). The pronounced

Table 5
Experimental details.

	I	II
Crystal data		
Chemical formula	$C_{21}H_{22}NO_3P$	$C_{21}H_{22}NOP$
M_r	367.38	335.39
Crystal system, space group	Orthorhombic, $P2_12_12_1$	Triclinic, $P1$
Temperature (K)	120	95
a, b, c (Å)	5.4947 (1), 8.1503 (1), 41.1096 (7)	9.0483 (7), 10.5533 (8), 11.0036 (6)
α, β, γ (°)	90, 90, 90	70.065 (6), 86.368 (5), 66.571 (7)
V (Å^3)	1841.03 (5)	903.15 (13)
Z	4	2
Radiation type	Cu $K\alpha$	Cu $K\alpha$
μ (mm^{-1})	1.49	1.39
Crystal size (mm)	0.90 × 0.27 × 0.07	0.62 × 0.09 × 0.07
Data collection		
Diffractometer	Oxford Diffraction Gemini	Oxford Diffraction SuperNova
Absorption correction	Multi-scan (*CrysAlis PRO*; Rigaku OD, 2017)	Multi-scan (*CrysAlis PRO*; Rigaku OD, 2017)
T_{min}, T_{max}	0.34, 0.90	0.49, 0.91
No. of measured, independent and observed [$I > 2.0\sigma(I)$] reflections	34246, 3356, 3262	15035, 6781, 6648
R_{int}	0.067	0.036
(sin $\theta/\lambda)_{max}$ (Å^{-1})	0.626	0.626
Refinement		
$R[F > 2\sigma(F)]$, $wR(F)$, S	0.037, 0.102, 1.02	0.034, 0.092, 0.97
No. of reflections	3355	6779
No. of parameters	240	443
No. of restraints	4	11
H-atom treatment	H atoms treated by a mixture of independent and constrained refinement	H atoms treated by a mixture of independent and constrained refinement
$\Delta\rho_{max}$, $\Delta\rho_{min}$ (e Å^{-3})	0.33, −0.38	0.49, −0.40
Absolute structure	Parsons *et al.* (2013), 1324 Friedel pairs	Parsons *et al.* (2013), 3140 Friedel pairs
Absolute structure parameter	0.013 (9)	−0.013 (7)

Computer programs: *CrysAlis PRO* (Rigaku OD, 2017), *SUPERFLIP* (Palatinus & Chapuis, 2007), *CRYSTALS* (Betteridge *et al.*, 2003), *JANA2006* (Petříček *et al.*, 2014), *Mercury* (Macrae *et al.*, 2020) and *MCE* (Rohlíček & Hušák, 2007).

differences are related to the contributions in the crystal packing by diastereotopic groups, especially in the C—H···π interactions, and the NMR chemical shifts of corresponding ^{13}C signals. The geometry parameters, conformations and NMR coupling constants of diastereotopic groups show minor differences (and/or similarities in some cases). In **I** with the $O_2P(O)N$ skeleton, the shorter P═O/P—N bonds and weaker N—H···O═P hydrogen bond are observed with respect to the structure **II** with the $C_2P(O)N$ skeleton. These structural features, resulting from different electronegativities of atoms, are reflected in the higher stretching frequencies of P═O and N—H bonds in the structure **I** (the latter because of a weaker N—H···O═P hydrogen bond). The lower volume/Z ratio of **II** is reflected by the crowding and observation of C···C contacts and raising H···H contacts, while **I** includes more H···O and O···C contacts. The study of analogous chiral structures retrieved from the CSD shows minor differences in bond lengths for diastereotopic P—C, P—O, and P—N bonds and more significant differences in torsion angles of diastereotopic groups.

8. Synthesis and crystallization

Preparation of $(C_6H_5O)_2P(O)[NH\text{-}(R)\text{-}(+)CH(C_2H_5)(C_6H_5)]$, (I). To a solution of $(C_6H_5O)_2P(O)Cl$ in dry chloroform, a solution of *R*-(+)-1-phenylpropylamine and triethylamine (1:1:1 molar ratio) in the same solvent was added at 273 K. After stirring for 4 h, the solvent was removed in a vacuum, and the obtained solid was washed with distilled water to remove $(C_2H_5)_3NHCl$. Colourless crystals were obtained from a solution of the title compound in $CHCl_3$/CH_3CN (1:2 *v*/*v*) after slow evaporation at room temperature.

Analytical data: IR (KBr, ν, cm^{-1}): 3268, 3063, 3029, 2970, 2929, 2854, 1592, 1492, 1453, 1420, 1244, 1200, 1167, 1058, 1020, 949, 900, 750, 689, 634, 579, 552, 520, 496, 457. ^{1}H NMR (400.22 MHz, $CDCl_3$): δ = 0.84 (*t*, *J* = 7.2 Hz, 3H), 1.81 (*m*, 2H), 3.84 (*t*, *J* = 10.8 Hz, 1H, NH), 4.32 (*m*, 1H), 6.99 (*d*, *J* = 8.4 Hz, 2H), 7.10 (*t*, *J* = 7.2 Hz, 1H), 7.16 – 7.35 (*m*, 12H); ^{13}C{^{1}H} NMR (100.64 MHz, $CDCl_3$): δ = 10.59, 31.80 (*d*, *J* = 8.1 Hz), 58.20, 120.12 (*d*, *J* = 4.0 Hz), 120.23 (*d*, *J* = 4.0 Hz), 124.63, 124.83, 126.50, 127.21, 128.44, 129.43, 129.64, 143.04 (*d*, *J* = 3.0 Hz), 150.74 (*d*, *J* = 7.0 Hz), 150.92 (*d*, *J* = 7.0 Hz); ^{31}P{^{1}H} NMR (162.01 MHz, $CDCl_3$): δ = −2.16.

Preparation of $(C_6H_5)_2P(O)[NH\text{-}(R)\text{-}(+)CH(C_2H_5)(C_6H_5)]$, (II). To a solution of $(C_6H_5)_2P(O)Cl$ in dry chloroform, a solution of *R*-(+)-1-phenylpropylamine and triethylamine (1:1:1 mole ratio) in the same solvent was added at 273 K. After stirring for 4 h, the solvent was removed in a vacuum, and the obtained solid was washed with distilled water to remove $(C_2H_5)_3NHCl$. Colourless crystals were obtained from a solution of the title compound in $CHCl_3$/CH_3CN (1:2 *v*/*v*) after slow evaporation at room temperature.

Analytical data: IR (KBr, ν, cm^{-1}): 3152, 3057, 3027, 2962, 2928, 2868, 1488, 1440, 1383, 1337, 1305, 1192, 1117, 1056, 1017, 929, 904, 838, 751, 721, 695, 603, 564, 533. ^{1}H NMR (400.22 MHz, DMSO-d_6): δ = 0.79 (*t*, *J* = 7.6 Hz, 3H), 1.69 (*m*, 1H), 1.82 (*m*, 1H), 3.84 (*m*, 1H), 5.91 (*t*, *J* = 10.2 Hz, 1H, NH), 7.26 (*m*, 5H), 7.37 (*m*, 2H), 7.50 (*m*, 4H), 7.64 (*m*, 2H), 7.79 (*m*, 2H); ^{13}C{^{1}H} NMR (100.64 MHz, DMSO-d_6): δ = 11.60, 32.62 (*d*, *J* = 4.7 Hz), 57.10, 126.87, 126.97, 128.45, 128.62 (*d*, *J* = 12.2 Hz), 128.82 (*d*, *J* = 12.1 Hz), 131.74 (*d*, *J* = 1.9 Hz), 131.86 (*d*, *J* = 2.1 Hz), 132.20 (*d*, *J* = 9.4 Hz), 132.38 (*d*, *J* = 9.5 Hz), 134.44 (*d*, *J* = 127.4 Hz), 134.77 (*d*, *J* = 126.4 Hz), 145.50 (*d*, *J* = 4.6 Hz); ^{31}P{^{1}H} NMR (162.01 MHz, DMSO-d_6): δ = 21.13.

9. Refinement

Crystal data, data collection and structure refinement details are summarized in Table 5. The H atoms were all located in difference-Fourier maps, but those attached to C atoms were repositioned geometrically. The H atoms were initially refined with soft restraints on the bond lengths and angles to regularize their geometries (C—H in the range 0.93–0.98 Å, N—H in the range 0.86–0.89 Å) and U_{iso}(H) values in the range 1.2–1.5×U_{eq} of the parent atom, after which the positions were refined with riding constraints (Cooper *et al.*, 2010; Watkin & Cooper, 2016). The absolute configuration was determined from the refinement of the Flack parameter (Parsons *et al.*, 2013).

Acknowledgements

The authors appreciatively acknowledge the Cambridge Crystallographic Data Centre for access to CSD Enterprise. Crystallography used the CzechNanoLab Research Infrastructure supported by MEYS CR (project LM2023051). Authors' contributions are as follows: Conceptualization, MP, FE and FS; methodology, FE, MP and FS; X-ray crystallography, MD and ES; investigation, FE and MP; writing (original draft), MP; writing (review and editing of the manuscript), MP, MD and ES; visualization, MP and ES; funding acquisition, FE and SB; resources, MD, ES, FE, FS and SB; supervision, MP, FS and SB.

References

Ahmadabad, F. K., Pourayoubi, M. & Bakhshi, H. (2019). *J. Appl. Polym. Sci.* **136**, 48034.
Akbari, S., Khoshnood, R. S., Ahmadabad, F. K., Pourayoubi, M., Dušek, M. & Shchegravina, E. S. (2019). *RSC Adv.* **9**, 9153–9159.
Betteridge, P. W., Carruthers, J. R., Cooper, R. I., Prout, K. & Watkin, D. J. (2003). *J. Appl. Cryst.* **36**, 1487.
Cooper, R. I., Thompson, A. L. & Watkin, D. J. (2010). *J. Appl. Cryst.* **43**, 1100–1107.
Corbridge, D. E. C. (2000). In *Phosphorus 2000: Chemistry, Biochemistry & Technology*, First ed. Amsterdam: Elsevier.
Cranwell, P. B., Hiscock, J. R., Haynes, C. J. E., Light, M. E., Wells, N. J. & Gale, P. A. (2013). *Chem. Commun.* **49**, 874–876.
Ferentinos, E., Xu, M., Grigoropoulos, A., Bratsos, I., Raptopoulou, C. P., Psycharis, V., Jiang, S.-D. & Kyritsis, P. (2019). *Inorg. Chem. Front.* **6**, 1405–1414.
Groom, C. R., Bruno, I. J., Lightfoot, M. P. & Ward, S. C. (2016). *Acta Cryst.* B**72**, 171–179.
Hamzehee, F., Pourayoubi, M., Farhadipour, A. & Choquesillo-Lazarte, D. (2017). *Phosphorus Sulfur Silicon*, **192**, 359–367.
Klare, H., Neudörfl, J. M. & Goldfuss, B. (2014). *Beilstein J. Org. Chem.* **10**, 224–236.
Liao, K., Hu, X.-S., Zhu, R.-Y., Rao, R.-H., Yu, J.-S., Zhou, F. & Zhou, J. (2019). *Chin. J. Chem.* **37**, 799–806.
Macrae, C. F., Sovago, I., Cottrell, S. J., Galek, P. T. A., McCabe, P., Pidcock, E., Platings, M., Shields, G. P., Stevens, J. S., Towler, M. & Wood, P. A. (2020). *J. Appl. Cryst.* **53**, 226–235.
Nakayama, K. & Thompson, W. J. (1990). *J. Am. Chem. Soc.* **112**, 6936–6942.
Nguyen, C. & Kim, A. (2008). *Macromol. Res.* **16**, 620–625.
Palacios, F., Alonso, C. & de los Santos, J. M. (2005). *Chem. Rev.* **105**, 899–932.
Palatinus, L. & Chapuis, G. (2007). *J. Appl. Cryst.* **40**, 786–790.
Parsons, S., Flack, H. D. & Wagner, T. (2013). *Acta Cryst.* B**69**, 249–259.
Petříček, V., Dušek, M. & Palatinus, L. (2014). *Z. Kristallogr.* **229**, 345–352.
Rigaku OD (2017). *CrysAlis PRO*. Rigaku Oxford Diffraction Ltd, Yarnton, England.
Rohlíček, J. & Hušák, M. (2007). *J. Appl. Cryst.* **40**, 600–601.
Sabbaghi, F., Pourayoubi, M., Nečas, M. & Damodaran, K. (2019). *Acta Cryst.* C**75**, 77–84.
Sabbaghi, F., Pourayoubi, M., Negari, M. & Nečas, M. (2011). *Acta Cryst.* E**67**, o2512.
Spackman, M. A. & Jayatilaka, D. (2009). *CrystEngComm*, **11**, 19–32.
Spackman, P. R., Turner, M. J., McKinnon, J. J., Wolff, S. K., Grimwood, D. J., Jayatilaka, D. & Spackman, M. A. (2021). *J. Appl. Cryst.* **54**, 1006–1011.
Sweeney, J. B., Cantrill, A. A., Drew, M. G. B., McLaren, A. B. & Thobhani, S. (2006). *Tetrahedron*, **62**, 3694–3703.
Taherzadeh, M., Pourayoubi, M., Vahdani Alviri, B., Shoghpour Bayraq, S., Ariani, M., Nečas, M., Dušek, M., Eigner, V., Amiri Rudbari, H., Bruno, G., Mancilla Percino, T., Leyva-Ramírez, M. A. & Damodaran, K. (2021). *Acta Cryst.* B**77**, 384–396.
Vahdani Alviri, B., Pourayoubi, M., Abdul Salam, A. A., Nečas, M., Lee, A. van der, Chithran, A. & Damodaran, K. (2020). *Acta Cryst.* C**76**, 104–116.
Wang, P., Douair, I., Zhao, Y., Wang, S., Zhu, J., Maron, L. & Zhu, C. (2021). *Angew. Chem. Int. Ed.* **60**, 473–479.
Warren, T. K., Jordan, R., Lo, M. K., Ray, A. S., Mackman, R. L., Soloveva, V., Siegel, D., Perron, M., Bannister, R., Hui, H. C., Larson, N., Strickley, R., Wells, J., Stuthman, K. S., Van Tongeren, S. A., Garza, N. L., Donnelly, G., Shurtleff, A. C., Retterer, C. J., Gharaibeh, D., Zamani, R., Kenny, T., Eaton, B. P., Grimes, E., Welch, L. S., Gomba, L., Wilhelmsen, C. L., Nichols, D. K., Nuss, J. E., Nagle, E. R., Kugelman, J. R., Palacios, G., Doerffler, E., Neville, S., Carra, E., Clarke, M. O., Zhang, L., Lew, W., Ross, B., Wang, Q., Chun, K., Wolfe, L., Babusis, D., Park, Y., Stray, K. M., Trancheva, I., Feng, J. Y., Barauskas, O., Xu, Y., Wong, P., Braun, M. R., Flint, M., McMullan, L. K., Chen, S. S., Fearns, R., Swaminathan, S., Mayers, D. L., Spiropoulou, C. F., Lee, W. A., Nichol, S. T., Cihlar, T. & Bavari, S. (2016). *Nature*, **531**, 381–385.
Watkin, D. J. & Cooper, R. I. (2016). *Acta Cryst.* B**72**, 661–683.
Wolff, S. K., Grimwood, D. J., McKinnon, J. J., Turner, M. J., Jayatilaka, D. & Spackman, M. A. (2013). *CrystalExplorer*. The University of Western Australia. http://crystalexplorer.scb.uwa.edu.au/.
Yin, L., Kanai, M. & Shibasaki, M. (2009). *J. Am. Chem. Soc.* **131**, 9610–9611.
Zhang, Y., Jia, A.-Q., Zhang, J.-J., Xin, Z. & Zhang, Q.-F. (2019). *J. Coord. Chem.* **72**, 1036–1048.

supporting information

Acta Cryst. (2023). E**79**, 769-776 [https://doi.org/10.1107/S2056989023006278]

Diastereotopic groups in two new single-enantiomer structures (R_2)P(O)[NH-(+)CH(C_2H_5)(C_6H_5)] (R = OC_6H_5 and C_6H_5)

Farnaz Eslami, Mehrdad Pourayoubi, Fahimeh Sabbaghi, Eliška Skořepová, Michal Dušek and Sahar Baniyaghoob

Computing details

For both structures, data collection: *CrysAlis PRO* (Rigaku OD, 2017); cell refinement: *CrysAlis PRO* (Rigaku OD, 2017); data reduction: *CrysAlis PRO* (Rigaku OD, 2017); program(s) used to solve structure: Superflip (Palatinus & Chapuis, 2007); program(s) used to refine structure: *CRYSTALS* (Betteridge *et al.*, 2003), *JANA2006* (Petricek *et al.*, 2014); molecular graphics: *Mercury* (Macrae *et al.*, 2020); software used to prepare material for publication: *CRYSTALS* (Betteridge *et al.*, 2003), *MCE* (Rohlicek & Husak, 2007).

Diphenyl [(*R*)-(+)-α-ethylbenzylamido]phosphate (I)

Crystal data

$C_{21}H_{22}NO_3P$
M_r = 367.38
Orthorhombic, $P2_12_12_1$
a = 5.4947 (1) Å
b = 8.1503 (1) Å
c = 41.1096 (7) Å
V = 1841.03 (5) Å^3
Z = 4
F(000) = 776
D_x = 1.325 Mg m^{-3}
Cu $K\alpha$ radiation, λ = 1.54180 Å
Cell parameters from 19519 reflections
θ = 4–68°
μ = 1.49 mm^{-1}
T = 120 K
Blade, clear colourless
0.90 × 0.27 × 0.07 mm

Data collection

Oxford Diffraction Gemini diffractometer
Graphite monochromator
ω scans
Absorption correction: multi-scan (CrysAlisPro; Rigaku OD, 2017)
T_{min} = 0.34, T_{max} = 0.90
34246 measured reflections
3356 independent reflections
3262 reflections with $I > 2.0\sigma(I)$
R_{int} = 0.067
θ_{max} = 74.9°, θ_{min} = 4.3°
h = −6→6
k = −9→9
l = −49→48

Refinement

Refinement on F^2
Least-squares matrix: full
$R[F > 3\sigma(F)]$ = 0.037
$wR(F)$ = 0.102
S = 1.02
3355 reflections
240 parameters
4 restraints
Primary atom site location: other
Hydrogen site location: difference Fourier map
H atoms treated by a mixture of independent and constrained refinement
Method = Modified Sheldrick $w = 1/[\sigma^2(F^2) + (0.03P)^2 + 3.0P]$, where $P = (\max(F_o^2,0) + 2F_c^2)/3$
$(\Delta/\sigma)_{max}$ = 0.001

$\Delta\rho_{max}$ = 0.33 e Å^{-3}
$\Delta\rho_{min}$ = −0.38 e Å^{-3}

Absolute structure: Parsons wt al. (2013), 1324 Friedel pairs
Absolute structure parameter: 0.013 (9)

Special details

Experimental. The crystal was placed in the cold stream of an Oxford Cryosystems open-flow nitrogen cryostat (Cosier & Glazer, 1986) with a nominal stability of 0.1K.
Cosier, J. & Glazer, A.M., 1986. J. Appl. Cryst. 105-107.

Refinement. X-ray analyses of **I** and **II** were performed on two different diffractometers, both using mirror-collimated Cu-*Kα* radiation (λ = 1.5418 Å), and CCD detector Atlas S2. The 120 K data set was acquired on a Gemini diffractometer with a classical sealed X-ray tube, while the 95 K data set was obtained on a SuperNova diffractometer with a micro-focus sealed tube. The data reduction and absorption correction were made with *CrysAlis PRO* software (Rigaku, 2017). The structures were solved by charge flipping methods using *SUPERFLIP* (Palatinus & Chapuis, 2007) software and refined by full-matrix least-squares on *F* squared value using Crystals (Betteridge *et al.*, 2003) and *JANA2006* (Petricek *et al.*, 2014) software programs. MCE (Rohlicek & Husak, 2007) software was used to visualize residual electron density maps.

Fractional atomic coordinates and isotropic or equivalent isotropic displacement parameters (Å^2)

	x	*y*	*z*	U_{iso}*/U_{eq}
P1	0.47169 (12)	0.71916 (8)	0.639453 (15)	0.0179
O2	0.4682 (3)	0.7590 (2)	0.60181 (4)	0.0229
C3	0.2732 (5)	0.8149 (3)	0.58334 (6)	0.0194
C4	0.0936 (5)	0.9153 (3)	0.59535 (7)	0.0218
C5	−0.0889 (5)	0.9701 (4)	0.57438 (7)	0.0264
C6	−0.0868 (6)	0.9248 (4)	0.54188 (7)	0.0274
C7	0.0950 (6)	0.8226 (4)	0.53038 (7)	0.0287
C8	0.2758 (5)	0.7663 (4)	0.55103 (6)	0.0244
O9	0.2348 (3)	0.6673 (2)	0.65240 (5)	0.0226
O10	0.5773 (4)	0.8880 (2)	0.65292 (4)	0.0221
C11	0.6063 (5)	0.9175 (3)	0.68651 (7)	0.0204
C12	0.8179 (5)	0.8689 (3)	0.70180 (7)	0.0232
C13	0.8488 (6)	0.9095 (4)	0.73416 (7)	0.0293
C14	0.6729 (6)	0.9975 (4)	0.75073 (7)	0.0323
C15	0.4628 (6)	1.0441 (4)	0.73500 (8)	0.0335
C16	0.4291 (6)	1.0050 (4)	0.70255 (7)	0.0284
N17	0.6906 (4)	0.5889 (3)	0.64476 (5)	0.0183
C18	0.6554 (5)	0.4134 (3)	0.63655 (7)	0.0190
C19	0.6338 (5)	0.3836 (3)	0.60013 (7)	0.0191
C20	0.8049 (6)	0.4457 (3)	0.57846 (7)	0.0236
C21	0.7840 (6)	0.4160 (4)	0.54532 (7)	0.0267
C22	0.5918 (6)	0.3231 (3)	0.53328 (7)	0.0265
C23	0.4216 (5)	0.2595 (4)	0.55459 (7)	0.0264
C24	0.4427 (5)	0.2905 (3)	0.58786 (6)	0.0230
C25	0.8638 (5)	0.3149 (3)	0.65162 (7)	0.0246
C26	0.8837 (6)	0.3359 (4)	0.68815 (7)	0.0306
H41	0.0953	0.9440	0.6176	0.0258*
H51	−0.2169	1.0378	0.5825	0.0333*
H61	−0.2126	0.9629	0.5284	0.0334*
H71	0.0971	0.7921	0.5081	0.0351*

H81	0.4006	0.6971	0.5432	0.0311*
H121	0.9407	0.8103	0.6910	0.0282*
H131	0.9901	0.8782	0.7449	0.0362*
H141	0.6962	1.0245	0.7732	0.0385*
H151	0.3406	1.1020	0.7466	0.0414*
H161	0.2869	1.0386	0.6919	0.0336*
H181	0.4995	0.3782	0.6465	0.0220*
H201	0.9339	0.5088	0.5863	0.0278*
H211	0.9021	0.4591	0.5309	0.0327*
H221	0.5809	0.3042	0.5105	0.0308*
H231	0.2889	0.1950	0.5464	0.0310*
H241	0.3217	0.2488	0.6018	0.0291*
H251	1.0183	0.3522	0.6420	0.0296*
H252	0.8302	0.1979	0.6470	0.0306*
H263	1.0151	0.2655	0.6967	0.0474*
H262	0.9199	0.4496	0.6934	0.0469*
H261	0.7302	0.3052	0.6981	0.0460*
H171	0.837 (3)	0.625 (2)	0.6445 (7)	0.0219 (19)*

Atomic displacement parameters (Å²)

	U^{11}	U^{22}	U^{33}	U^{12}	U^{13}	U^{23}
P1	0.0183 (3)	0.0169 (3)	0.0184 (3)	0.0003 (3)	0.0003 (3)	−0.0009 (3)
O2	0.0178 (9)	0.0304 (10)	0.0207 (9)	0.0051 (9)	0.0004 (8)	0.0012 (7)
C3	0.0166 (13)	0.0204 (14)	0.0212 (13)	0.0002 (11)	−0.0014 (10)	0.0027 (10)
C4	0.0241 (15)	0.0203 (13)	0.0209 (13)	−0.0005 (12)	0.0004 (12)	−0.0009 (11)
C5	0.0215 (15)	0.0214 (14)	0.0364 (16)	0.0047 (12)	0.0003 (13)	0.0024 (12)
C6	0.0241 (15)	0.0249 (15)	0.0331 (16)	−0.0028 (12)	−0.0096 (13)	0.0053 (12)
C7	0.0328 (17)	0.0320 (16)	0.0213 (14)	−0.0007 (13)	−0.0056 (12)	0.0009 (12)
C8	0.0246 (14)	0.0262 (15)	0.0224 (13)	0.0035 (12)	0.0018 (11)	0.0007 (11)
O9	0.0194 (10)	0.0225 (10)	0.0259 (9)	0.0001 (8)	0.0017 (8)	−0.0009 (8)
O10	0.0248 (10)	0.0183 (9)	0.0233 (9)	−0.0007 (8)	−0.0009 (8)	−0.0003 (8)
C11	0.0222 (14)	0.0154 (12)	0.0235 (13)	−0.0048 (11)	0.0023 (11)	−0.0024 (11)
C12	0.0244 (15)	0.0221 (14)	0.0232 (14)	−0.0012 (12)	0.0029 (12)	−0.0018 (11)
C13	0.0314 (16)	0.0315 (16)	0.0252 (15)	−0.0041 (14)	−0.0009 (13)	0.0024 (13)
C14	0.0430 (19)	0.0289 (16)	0.0251 (15)	−0.0109 (15)	0.0066 (14)	−0.0058 (13)
C15	0.0321 (17)	0.0298 (16)	0.0385 (17)	−0.0019 (14)	0.0098 (15)	−0.0117 (13)
C16	0.0239 (15)	0.0232 (14)	0.0380 (16)	0.0030 (13)	0.0011 (13)	−0.0046 (12)
N17	0.0173 (11)	0.0173 (11)	0.0204 (12)	−0.0029 (9)	−0.0010 (10)	−0.0020 (9)
C18	0.0209 (13)	0.0146 (12)	0.0215 (13)	−0.0010 (11)	0.0033 (11)	−0.0024 (11)
C19	0.0204 (13)	0.0138 (13)	0.0230 (13)	0.0030 (11)	0.0017 (11)	−0.0028 (10)
C20	0.0235 (15)	0.0211 (14)	0.0261 (14)	−0.0029 (12)	0.0015 (12)	−0.0018 (11)
C21	0.0282 (16)	0.0245 (15)	0.0275 (15)	0.0017 (13)	0.0069 (13)	0.0021 (12)
C22	0.0339 (17)	0.0265 (15)	0.0191 (13)	0.0081 (13)	−0.0017 (12)	−0.0018 (11)
C23	0.0232 (15)	0.0270 (15)	0.0288 (14)	0.0019 (12)	−0.0056 (12)	−0.0075 (12)
C24	0.0211 (13)	0.0225 (13)	0.0254 (13)	0.0020 (13)	0.0020 (11)	−0.0004 (12)
C25	0.0295 (15)	0.0183 (14)	0.0261 (14)	0.0034 (12)	−0.0001 (12)	0.0018 (11)
C26	0.0413 (18)	0.0226 (15)	0.0279 (15)	0.0024 (14)	−0.0047 (13)	0.0016 (12)

Geometric parameters (Å, º)

P1—O2	1.5814 (18)	C15—C16	1.384 (4)
P1—O9	1.469 (2)	C15—H151	0.948
P1—O10	1.5924 (19)	C16—H161	0.937
P1—N17	1.619 (2)	N17—C18	1.482 (3)
O2—C3	1.390 (3)	N17—H171	0.854 (17)
C3—C4	1.373 (4)	C18—C19	1.522 (4)
C3—C8	1.386 (4)	C18—C25	1.530 (4)
C4—C5	1.396 (4)	C18—H181	0.991
C4—H41	0.945	C19—C20	1.391 (4)
C5—C6	1.386 (4)	C19—C24	1.390 (4)
C5—H51	0.954	C20—C21	1.388 (4)
C6—C7	1.383 (4)	C20—H201	0.933
C6—H61	0.939	C21—C22	1.390 (4)
C7—C8	1.385 (4)	C21—H211	0.946
C7—H71	0.948	C22—C23	1.383 (4)
C8—H81	0.945	C22—H221	0.953
O10—C11	1.411 (3)	C23—C24	1.396 (4)
C11—C12	1.380 (4)	C23—H231	0.960
C11—C16	1.375 (4)	C24—H241	0.940
C12—C13	1.382 (4)	C25—C26	1.516 (4)
C12—H121	0.938	C25—H251	0.985
C13—C14	1.383 (5)	C25—H252	0.989
C13—H131	0.929	C26—H263	0.987
C14—C15	1.377 (5)	C26—H262	0.972
C14—H141	0.959	C26—H261	0.970
O2—P1—O9	113.77 (11)	C15—C16—H161	119.7
O2—P1—O10	99.62 (10)	C11—C16—H161	121.2
O9—P1—O10	116.45 (11)	P1—N17—C18	120.34 (18)
O2—P1—N17	106.00 (11)	P1—N17—H171	118.2 (12)
O9—P1—N17	114.90 (12)	C18—N17—H171	116.6 (12)
O10—P1—N17	104.43 (11)	N17—C18—C19	112.8 (2)
P1—O2—C3	127.68 (17)	N17—C18—C25	108.4 (2)
O2—C3—C4	123.5 (2)	C19—C18—C25	111.9 (2)
O2—C3—C8	114.9 (2)	N17—C18—H181	107.4
C4—C3—C8	121.5 (3)	C19—C18—H181	107.0
C3—C4—C5	119.0 (3)	C25—C18—H181	109.2
C3—C4—H41	119.3	C18—C19—C20	121.3 (2)
C5—C4—H41	121.7	C18—C19—C24	120.2 (2)
C4—C5—C6	120.3 (3)	C20—C19—C24	118.5 (3)
C4—C5—H51	120.0	C19—C20—C21	120.6 (3)
C6—C5—H51	119.7	C19—C20—H201	119.6
C5—C6—C7	119.7 (3)	C21—C20—H201	119.8
C5—C6—H61	118.4	C20—C21—C22	120.5 (3)
C7—C6—H61	121.9	C20—C21—H211	119.5
C6—C7—C8	120.5 (3)	C22—C21—H211	120.1

C6—C7—H71	119.7	C21—C22—C23	119.5 (3)
C8—C7—H71	119.7	C21—C22—H221	119.1
C3—C8—C7	119.0 (3)	C23—C22—H221	121.4
C3—C8—H81	120.3	C22—C23—C24	119.8 (3)
C7—C8—H81	120.7	C22—C23—H231	119.7
P1—O10—C11	121.91 (16)	C24—C23—H231	120.5
O10—C11—C12	119.5 (2)	C23—C24—C19	121.1 (3)
O10—C11—C16	118.5 (3)	C23—C24—H241	118.1
C12—C11—C16	121.8 (3)	C19—C24—H241	120.7
C11—C12—C13	118.2 (3)	C18—C25—C26	113.3 (2)
C11—C12—H121	122.5	C18—C25—H251	108.7
C13—C12—H121	119.3	C26—C25—H251	107.6
C12—C13—C14	120.9 (3)	C18—C25—H252	106.8
C12—C13—H131	119.6	C26—C25—H252	108.1
C14—C13—H131	119.5	H251—C25—H252	112.4
C13—C14—C15	119.8 (3)	C25—C26—H263	110.0
C13—C14—H141	120.0	C25—C26—H262	109.9
C15—C14—H141	120.1	H263—C26—H262	109.0
C14—C15—C16	120.1 (3)	C25—C26—H261	109.0
C14—C15—H151	119.7	H263—C26—H261	109.6
C16—C15—H151	120.2	H262—C26—H261	109.3
C15—C16—C11	119.1 (3)		

Hydrogen-bond geometry (Å, º)

D—H···*A*	*D*—H	H···*A*	*D*···*A*	*D*—H···*A*
C12—H121···O9^{i}	0.94	2.55	3.474 (4)	170
N17—H171···O9^{i}	0.85	2.24	3.074 (4)	166 (2)

Symmetry code: (i) *x*+1, *y*, *z*.

N-[(*R*)-(+)-α-Ethylbenzyl]-*P*,*P*-diphenylphosphinic amide (II)

Crystal data

$C_{21}H_{22}NOP$
M_r = 335.39
Triclinic, *P*1
a = 9.0483 (7) Å
b = 10.5533 (8) Å
c = 11.0036 (6) Å
α = 70.065 (6)°
β = 86.368 (5)°
γ = 66.571 (7)°
V = 903.15 (13) Å^3

Z = 2
F(000) = 356
D_x = 1.233 Mg m^{-3}
Cu *Kα* radiation, λ = 1.54180 Å
Cell parameters from 11237 reflections
θ = 4–74°
μ = 1.39 mm^{-1}
T = 95 K
Needle, colorless
0.62 × 0.09 × 0.07 mm

Data collection

Oxford Diffraction SuperNova diffractometer
Focussing mirrors monochromator
ω scans

Absorption correction: multi-scan (CrysAlisPro; Rigaku OD, 2017)
T_{min} = 0.49, T_{max} = 0.91
15035 measured reflections
6781 independent reflections

6648 reflections with $I > 2.0\sigma(I)$
$R_{int} = 0.036$
$\theta_{max} = 74.8°$, $\theta_{min} = 4.3°$

$h = -10 \rightarrow 11$
$k = -13 \rightarrow 13$
$l = -13 \rightarrow 13$

Refinement

Refinement on F^2
Least-squares matrix: full
$R[F > 3\sigma(F)] = 0.034$
$wR(F) = 0.092$
$S = 0.97$
6779 reflections
443 parameters
11 restraints
Primary atom site location: other
Hydrogen site location: difference Fourier map
H atoms treated by a mixture of independent and constrained refinement

Method = Modified Sheldrick $w = 1/[\sigma^2(F^2) + (0.05P)^2 + 0.53P]$, where $P = (\max(F_o^2,0) + 2F_c^2)/3$
$(\Delta/\sigma)_{max} = 0.001$
$\Delta\rho_{max} = 0.49$ e Å^{-3}
$\Delta\rho_{min} = -0.40$ e Å^{-3}
Extinction correction: Larson (1970), Equation 22
Extinction coefficient: 12 (2)
Absolute structure: Parsons *et al.* (2013), 3140 Friedel pairs
Absolute structure parameter: −0.013 (7)

Special details

Experimental. The crystal was placed in the cold stream of an Oxford Cryosystems open-flow nitrogen cryostat (Cosier & Glazer, 1986) with a nominal stability of 0.1K.
Cosier, J. & Glazer, A.M., 1986. J. Appl. Cryst. 105-107.

Fractional atomic coordinates and isotropic or equivalent isotropic displacement parameters (Å²)

	x	*y*	*z*	U_{iso}*/U_{eq}
P1	0.65963 (7)	0.68073 (7)	0.14489 (6)	0.0147
O2	0.68651 (18)	0.78920 (16)	0.18817 (15)	0.0192
N3	0.5062 (2)	0.7351 (2)	0.04120 (17)	0.0183
C4	0.4906 (3)	0.8436 (2)	−0.0895 (2)	0.0186
C5	0.4419 (3)	0.7964 (2)	−0.1908 (2)	0.0200
C6	0.3292 (3)	0.7336 (2)	−0.1687 (2)	0.0246
C7	0.2863 (3)	0.6919 (3)	−0.2628 (3)	0.0311
C8	0.3541 (3)	0.7134 (3)	−0.3805 (3)	0.0375
C9	0.4638 (3)	0.7781 (3)	−0.4047 (3)	0.0358
C10	0.5082 (3)	0.8189 (3)	−0.3100 (2)	0.0280
C11	0.3751 (3)	0.9980 (2)	−0.0941 (2)	0.0224
C12	0.3668 (3)	1.1186 (3)	−0.2214 (2)	0.0301
C13	0.6291 (3)	0.5395 (2)	0.2788 (2)	0.0171
C14	0.5864 (3)	0.4341 (2)	0.2599 (2)	0.0231
C15	0.5756 (3)	0.3206 (3)	0.3661 (3)	0.0283
C16	0.6061 (3)	0.3133 (3)	0.4908 (2)	0.0326
C17	0.6464 (3)	0.4184 (3)	0.5101 (2)	0.0339
C18	0.6596 (3)	0.5315 (3)	0.4045 (2)	0.0244
C19	0.8355 (3)	0.5873 (2)	0.0723 (2)	0.0163
C20	0.9871 (3)	0.5761 (2)	0.1080 (2)	0.0228
C21	1.1249 (3)	0.4987 (3)	0.0594 (3)	0.0291
C22	1.1132 (3)	0.4300 (3)	−0.0238 (3)	0.0370
C23	0.9630 (4)	0.4415 (3)	−0.0610 (3)	0.0366
C24	0.8248 (3)	0.5197 (3)	−0.0129 (2)	0.0266
P25	0.07166 (8)	0.86743 (7)	0.21332 (6)	0.0153

O26	0.19971 (18)	0.79311 (17)	0.13860 (15)	0.0191
N27	−0.1158 (2)	0.9595 (2)	0.14867 (17)	0.0186
C28	−0.1622 (3)	1.0887 (2)	0.0291 (2)	0.0190
C29	−0.1193 (3)	1.0513 (2)	−0.0942 (2)	0.0181
C30	−0.0560 (3)	1.1317 (3)	−0.1945 (2)	0.0246
C31	−0.0237 (3)	1.1016 (3)	−0.3093 (2)	0.0284
C32	−0.0532 (3)	0.9893 (3)	−0.3247 (2)	0.0273
C33	−0.1146 (3)	0.9065 (3)	−0.2249 (2)	0.0255
C34	−0.1478 (3)	0.9383 (2)	−0.1108 (2)	0.0217
C35	−0.3445 (3)	1.1792 (2)	0.0259 (2)	0.0236
C36	−0.4123 (3)	1.3159 (3)	−0.0958 (3)	0.0292
C37	0.0538 (3)	0.7326 (2)	0.3613 (2)	0.0170
C38	0.1730 (3)	0.5907 (2)	0.3955 (2)	0.0199
C39	0.1665 (3)	0.4812 (3)	0.5077 (2)	0.0262
C40	0.0416 (3)	0.5138 (3)	0.5867 (2)	0.0262
C41	−0.0766 (3)	0.6557 (3)	0.5537 (2)	0.0258
C42	−0.0719 (3)	0.7651 (2)	0.4412 (2)	0.0216
C43	0.1205 (3)	0.9967 (2)	0.2565 (2)	0.0189
C44	0.2809 (3)	0.9847 (2)	0.2533 (2)	0.0212
C45	0.3232 (3)	1.0805 (3)	0.2895 (2)	0.0264
C46	0.2078 (3)	1.1884 (3)	0.3291 (2)	0.0277
C47	0.0476 (3)	1.2019 (2)	0.3324 (2)	0.0243
C48	0.0055 (3)	1.1064 (2)	0.2959 (2)	0.0209
H41	0.5974	0.8444	−0.1091	0.0220*
H61	0.2795	0.7205	−0.0895	0.0305*
H71	0.2113	0.6464	−0.2449	0.0358*
H81	0.3236	0.6870	−0.4464	0.0453*
H91	0.5092	0.7947	−0.4848	0.0425*
H101	0.5834	0.8620	−0.3268	0.0343*
H111	0.2680	0.9967	−0.0769	0.0261*
H112	0.4090	1.0174	−0.0231	0.0257*
H121	0.2982	1.2149	−0.2168	0.0438*
H122	0.3213	1.1064	−0.2928	0.0436*
H123	0.4734	1.1161	−0.2430	0.0437*
H141	0.5650	0.4389	0.1758	0.0280*
H151	0.5505	0.2486	0.3538	0.0328*
H161	0.6024	0.2356	0.5624	0.0404*
H171	0.6628	0.4139	0.5962	0.0414*
H181	0.6884	0.6026	0.4173	0.0270*
H201	0.9926	0.6245	0.1670	0.0274*
H211	1.2268	0.4921	0.0852	0.0351*
H221	1.2068	0.3769	−0.0554	0.0433*
H231	0.9537	0.3961	−0.1187	0.0442*
H241	0.7251	0.5273	−0.0381	0.0319*
H281	−0.1033	1.1485	0.0335	0.0213*
H301	−0.0382	1.2104	−0.1855	0.0287*
H311	0.0176	1.1593	−0.3771	0.0337*
H321	−0.0304	0.9685	−0.4040	0.0327*

H331	−0.1283	0.8249	−0.2332	0.0317*
H341	−0.1856	0.8793	−0.0420	0.0267*
H352	−0.4011	1.1147	0.0318	0.0272*
H351	−0.3627	1.2111	0.1016	0.0271*
H362	−0.5227	1.3761	−0.0867	0.0432*
H361	−0.4124	1.2855	−0.1701	0.0425*
H363	−0.3466	1.3730	−0.1133	0.0432*
H381	0.2588	0.5680	0.3428	0.0238*
H391	0.2475	0.3849	0.5279	0.0309*
H401	0.0361	0.4387	0.6628	0.0323*
H411	−0.1604	0.6800	0.6071	0.0306*
H421	−0.1508	0.8603	0.4175	0.0247*
H441	0.3606	0.9101	0.2267	0.0238*
H451	0.4286	1.0731	0.2856	0.0318*
H461	0.2360	1.2529	0.3533	0.0341*
H471	−0.0304	1.2756	0.3581	0.0302*
H481	−0.1012	1.1142	0.2988	0.0256*
H271	−0.169 (2)	0.907 (2)	0.159 (2)	0.0223 (19)*
H31	0.417 (2)	0.746 (2)	0.0763 (17)	0.0229 (19)*

Atomic displacement parameters (Å²)

	U^{11}	U^{22}	U^{33}	U^{12}	U^{13}	U^{23}
P1	0.0160 (2)	0.0161 (2)	0.0131 (2)	−0.0080 (2)	0.00316 (19)	−0.00467 (19)
O2	0.0189 (7)	0.0201 (7)	0.0238 (8)	−0.0108 (6)	0.0052 (6)	−0.0110 (6)
N3	0.0187 (9)	0.0216 (9)	0.0146 (8)	−0.0111 (7)	0.0048 (7)	−0.0032 (7)
C4	0.0205 (11)	0.0233 (10)	0.0133 (10)	−0.0131 (9)	0.0033 (8)	−0.0029 (8)
C5	0.0182 (10)	0.0200 (10)	0.0175 (10)	−0.0056 (8)	−0.0008 (8)	−0.0034 (8)
C6	0.0256 (12)	0.0231 (11)	0.0242 (11)	−0.0097 (10)	−0.0016 (9)	−0.0064 (9)
C7	0.0285 (13)	0.0254 (12)	0.0378 (14)	−0.0069 (10)	−0.0096 (11)	−0.0114 (11)
C8	0.0388 (16)	0.0336 (14)	0.0335 (14)	−0.0003 (12)	−0.0143 (12)	−0.0176 (12)
C9	0.0352 (15)	0.0427 (15)	0.0233 (12)	−0.0044 (12)	−0.0001 (11)	−0.0170 (11)
C10	0.0258 (12)	0.0350 (13)	0.0194 (11)	−0.0093 (10)	0.0028 (9)	−0.0083 (10)
C11	0.0272 (12)	0.0213 (11)	0.0186 (11)	−0.0121 (9)	0.0014 (9)	−0.0040 (9)
C12	0.0397 (14)	0.0233 (12)	0.0225 (12)	−0.0141 (11)	−0.0003 (10)	0.0001 (10)
C13	0.0144 (10)	0.0177 (10)	0.0171 (10)	−0.0054 (8)	0.0031 (8)	−0.0051 (8)
C14	0.0205 (11)	0.0238 (11)	0.0248 (11)	−0.0097 (9)	0.0071 (9)	−0.0079 (9)
C15	0.0253 (12)	0.0183 (11)	0.0378 (14)	−0.0108 (9)	0.0103 (10)	−0.0042 (10)
C16	0.0266 (12)	0.0243 (12)	0.0279 (13)	−0.0050 (10)	0.0102 (10)	0.0060 (10)
C17	0.0347 (14)	0.0377 (14)	0.0159 (11)	−0.0096 (11)	0.0062 (10)	0.0002 (10)
C18	0.0272 (12)	0.0258 (11)	0.0187 (11)	−0.0090 (10)	0.0015 (9)	−0.0081 (9)
C19	0.0165 (10)	0.0156 (9)	0.0161 (10)	−0.0077 (8)	0.0061 (8)	−0.0042 (8)
C20	0.0228 (11)	0.0210 (11)	0.0228 (11)	−0.0086 (9)	0.0035 (9)	−0.0059 (9)
C21	0.0209 (12)	0.0276 (12)	0.0373 (14)	−0.0124 (10)	0.0089 (10)	−0.0073 (11)
C22	0.0331 (14)	0.0324 (14)	0.0502 (17)	−0.0149 (11)	0.0257 (13)	−0.0216 (13)
C23	0.0477 (17)	0.0424 (15)	0.0403 (15)	−0.0287 (13)	0.0258 (13)	−0.0298 (13)
C24	0.0326 (13)	0.0336 (13)	0.0270 (12)	−0.0223 (11)	0.0116 (10)	−0.0171 (10)
P25	0.0168 (3)	0.0172 (2)	0.0135 (2)	−0.0086 (2)	0.00278 (19)	−0.00540 (19)

O26	0.0208 (8)	0.0215 (7)	0.0173 (7)	−0.0112 (6)	0.0044 (6)	−0.0068 (6)
N27	0.0201 (9)	0.0207 (9)	0.0179 (9)	−0.0133 (8)	0.0021 (7)	−0.0043 (7)
C28	0.0222 (11)	0.0156 (10)	0.0183 (10)	−0.0091 (8)	−0.0003 (8)	−0.0026 (8)
C29	0.0162 (10)	0.0167 (9)	0.0192 (10)	−0.0068 (8)	−0.0006 (8)	−0.0030 (8)
C30	0.0288 (12)	0.0226 (11)	0.0233 (11)	−0.0142 (10)	0.0007 (10)	−0.0040 (9)
C31	0.0291 (12)	0.0342 (13)	0.0165 (10)	−0.0147 (11)	0.0007 (9)	0.0002 (9)
C32	0.0240 (12)	0.0327 (13)	0.0183 (11)	−0.0056 (10)	0.0000 (9)	−0.0073 (10)
C33	0.0259 (12)	0.0293 (12)	0.0250 (12)	−0.0125 (10)	0.0028 (10)	−0.0120 (10)
C34	0.0226 (11)	0.0250 (11)	0.0201 (11)	−0.0132 (9)	0.0042 (9)	−0.0069 (9)
C35	0.0237 (12)	0.0228 (11)	0.0259 (12)	−0.0096 (9)	0.0015 (9)	−0.0099 (9)
C36	0.0240 (12)	0.0218 (11)	0.0359 (14)	−0.0056 (10)	−0.0056 (10)	−0.0058 (10)
C37	0.0187 (10)	0.0215 (10)	0.0152 (9)	−0.0113 (8)	0.0000 (8)	−0.0075 (8)
C38	0.0201 (11)	0.0220 (11)	0.0181 (10)	−0.0091 (9)	0.0040 (8)	−0.0070 (9)
C39	0.0303 (13)	0.0199 (11)	0.0216 (11)	−0.0085 (10)	0.0028 (9)	−0.0012 (9)
C40	0.0331 (13)	0.0263 (12)	0.0170 (10)	−0.0155 (10)	0.0023 (10)	−0.0005 (9)
C41	0.0258 (12)	0.0318 (12)	0.0199 (11)	−0.0125 (10)	0.0078 (9)	−0.0087 (9)
C42	0.0230 (11)	0.0224 (11)	0.0200 (11)	−0.0096 (9)	0.0032 (9)	−0.0076 (9)
C43	0.0221 (11)	0.0182 (10)	0.0142 (9)	−0.0069 (8)	0.0026 (8)	−0.0047 (8)
C44	0.0200 (11)	0.0258 (11)	0.0198 (11)	−0.0115 (9)	0.0025 (9)	−0.0074 (9)
C45	0.0259 (12)	0.0289 (12)	0.0321 (13)	−0.0177 (10)	0.0013 (10)	−0.0117 (10)
C46	0.0379 (14)	0.0257 (12)	0.0261 (12)	−0.0186 (11)	−0.0003 (10)	−0.0093 (10)
C47	0.0296 (13)	0.0207 (11)	0.0238 (11)	−0.0089 (9)	0.0038 (9)	−0.0108 (9)
C48	0.0226 (11)	0.0220 (10)	0.0187 (10)	−0.0112 (9)	0.0035 (9)	−0.0055 (8)

Geometric parameters (Å, º)

P1—O2	1.4846 (15)	P25—O26	1.4933 (15)
P1—N3	1.6367 (19)	P25—N27	1.6426 (19)
P1—C13	1.802 (2)	P25—C37	1.808 (2)
P1—C19	1.808 (2)	P25—C43	1.797 (2)
N3—C4	1.474 (2)	N27—C28	1.469 (3)
N3—H31	0.856 (16)	N27—H271	0.841 (16)
C4—C5	1.517 (3)	C28—C29	1.524 (3)
C4—C11	1.532 (3)	C28—C35	1.538 (3)
C4—H41	0.980	C28—H281	0.988
C5—C6	1.391 (3)	C29—C30	1.391 (3)
C5—C10	1.391 (3)	C29—C34	1.386 (3)
C6—C7	1.383 (3)	C30—C31	1.391 (3)
C6—H61	0.948	C30—H301	0.944
C7—C8	1.383 (4)	C31—C32	1.378 (4)
C7—H71	0.953	C31—H311	0.951
C8—C9	1.380 (4)	C32—C33	1.390 (3)
C8—H81	0.950	C32—H321	0.961
C9—C10	1.389 (4)	C33—C34	1.392 (3)
C9—H91	0.940	C33—H331	0.952
C10—H101	0.936	C34—H341	0.945
C11—C12	1.520 (3)	C35—C36	1.527 (3)
C11—H111	0.980	C35—H352	0.986

C11—H112	0.967	C35—H351	0.982
C12—H121	0.975	C36—H362	0.968
C12—H122	0.977	C36—H361	0.975
C12—H123	0.971	C36—H363	0.972
C13—C14	1.393 (3)	C37—C38	1.390 (3)
C13—C18	1.395 (3)	C37—C42	1.397 (3)
C14—C15	1.390 (3)	C38—C39	1.391 (3)
C14—H141	0.938	C38—H381	0.941
C15—C16	1.387 (4)	C39—C40	1.387 (3)
C15—H151	0.928	C39—H391	0.945
C16—C17	1.379 (4)	C40—C41	1.387 (3)
C16—H161	0.934	C40—H401	0.952
C17—C18	1.392 (3)	C41—C42	1.387 (3)
C17—H171	0.949	C41—H411	0.937
C18—H181	0.940	C42—H421	0.929
C19—C20	1.399 (3)	C43—C44	1.406 (3)
C19—C24	1.387 (3)	C43—C48	1.392 (3)
C20—C21	1.383 (3)	C44—C45	1.389 (3)
C20—H201	0.967	C44—H441	0.950
C21—C22	1.379 (4)	C45—C46	1.382 (4)
C21—H211	0.951	C45—H451	0.925
C22—C23	1.391 (4)	C46—C47	1.398 (4)
C22—H221	0.933	C46—H461	0.932
C23—C24	1.384 (3)	C47—C48	1.388 (3)
C23—H231	0.942	C47—H471	0.933
C24—H241	0.925	C48—H481	0.935

O2—P1—N3	119.94 (9)	O26—P25—N27	119.61 (9)
O2—P1—C13	111.80 (9)	O26—P25—C37	109.99 (9)
N3—P1—C13	102.43 (10)	N27—P25—C37	102.69 (10)
O2—P1—C19	110.23 (9)	O26—P25—C43	110.87 (9)
N3—P1—C19	105.15 (10)	N27—P25—C43	104.84 (10)
C13—P1—C19	106.21 (9)	C37—P25—C43	108.07 (10)
P1—N3—C4	120.91 (14)	P25—N27—C28	122.16 (15)
P1—N3—H31	113.3 (12)	P25—N27—H271	114.1 (12)
C4—N3—H31	114.3 (12)	C28—N27—H271	115.3 (12)
N3—C4—C5	110.46 (17)	N27—C28—C29	114.02 (17)
N3—C4—C11	110.64 (17)	N27—C28—C35	107.53 (17)
C5—C4—C11	113.02 (18)	C29—C28—C35	111.51 (18)
N3—C4—H41	108.1	N27—C28—H281	108.1
C5—C4—H41	106.1	C29—C28—H281	106.9
C11—C4—H41	108.3	C35—C28—H281	108.7
C4—C5—C6	121.51 (19)	C28—C29—C30	121.5 (2)
C4—C5—C10	119.7 (2)	C28—C29—C34	120.35 (19)
C6—C5—C10	118.8 (2)	C30—C29—C34	118.2 (2)
C5—C6—C7	120.4 (2)	C29—C30—C31	121.3 (2)
C5—C6—H61	120.3	C29—C30—H301	119.1
C7—C6—H61	119.3	C31—C30—H301	119.5

C6—C7—C8	120.3 (3)	C30—C31—C32	119.9 (2)
C6—C7—H71	119.1	C30—C31—H311	119.8
C8—C7—H71	120.5	C32—C31—H311	120.3
C7—C8—C9	119.8 (2)	C31—C32—C33	119.6 (2)
C7—C8—H81	120.9	C31—C32—H321	119.7
C9—C8—H81	119.2	C33—C32—H321	120.7
C8—C9—C10	120.0 (2)	C32—C33—C34	120.1 (2)
C8—C9—H91	120.5	C32—C33—H331	119.6
C10—C9—H91	119.5	C34—C33—H331	120.2
C5—C10—C9	120.6 (3)	C33—C34—C29	120.9 (2)
C5—C10—H101	120.0	C33—C34—H341	119.7
C9—C10—H101	119.4	C29—C34—H341	119.3
C4—C11—C12	113.76 (19)	C28—C35—C36	113.74 (19)
C4—C11—H111	107.7	C28—C35—H352	108.0
C12—C11—H111	110.6	C36—C35—H352	109.3
C4—C11—H112	108.3	C28—C35—H351	107.8
C12—C11—H112	109.8	C36—C35—H351	108.2
H111—C11—H112	106.4	H352—C35—H351	109.8
C11—C12—H121	110.4	C35—C36—H362	110.1
C11—C12—H122	110.6	C35—C36—H361	109.1
H121—C12—H122	108.0	H362—C36—H361	108.1
C11—C12—H123	111.5	C35—C36—H363	111.5
H121—C12—H123	109.3	H362—C36—H363	110.1
H122—C12—H123	106.9	H361—C36—H363	107.8
P1—C13—C14	121.84 (17)	P25—C37—C38	117.22 (16)
P1—C13—C18	118.28 (17)	P25—C37—C42	123.28 (17)
C14—C13—C18	119.8 (2)	C38—C37—C42	119.5 (2)
C13—C14—C15	120.0 (2)	C37—C38—C39	120.3 (2)
C13—C14—H141	120.4	C37—C38—H381	120.1
C15—C14—H141	119.6	C39—C38—H381	119.6
C14—C15—C16	119.9 (2)	C38—C39—C40	120.0 (2)
C14—C15—H151	120.2	C38—C39—H391	118.8
C16—C15—H151	119.9	C40—C39—H391	121.2
C15—C16—C17	120.3 (2)	C39—C40—C41	119.9 (2)
C15—C16—H161	120.3	C39—C40—H401	120.1
C17—C16—H161	119.4	C41—C40—H401	120.1
C16—C17—C18	120.2 (2)	C40—C41—C42	120.4 (2)
C16—C17—H171	119.2	C40—C41—H411	120.9
C18—C17—H171	120.5	C42—C41—H411	118.7
C13—C18—C17	119.7 (2)	C37—C42—C41	119.9 (2)
C13—C18—H181	119.8	C37—C42—H421	118.8
C17—C18—H181	120.5	C41—C42—H421	121.3
P1—C19—C20	119.48 (17)	P25—C43—C44	118.93 (17)
P1—C19—C24	121.36 (18)	P25—C43—C48	122.26 (18)
C20—C19—C24	119.1 (2)	C44—C43—C48	118.8 (2)
C19—C20—C21	120.8 (2)	C43—C44—C45	120.2 (2)
C19—C20—H201	118.2	C43—C44—H441	119.6
C21—C20—H201	121.0	C45—C44—H441	120.1

C20—C21—C22	119.6 (2)	C44—C45—C46	120.3 (2)
C20—C21—H211	119.4	C44—C45—H451	119.7
C22—C21—H211	120.9	C46—C45—H451	120.0
C21—C22—C23	120.1 (2)	C45—C46—C47	120.1 (2)
C21—C22—H221	119.2	C45—C46—H461	120.4
C23—C22—H221	120.7	C47—C46—H461	119.5
C22—C23—C24	120.3 (2)	C46—C47—C48	119.6 (2)
C22—C23—H231	120.7	C46—C47—H471	120.0
C24—C23—H231	119.1	C48—C47—H471	120.4
C19—C24—C23	120.1 (2)	C43—C48—C47	121.0 (2)
C19—C24—H241	119.9	C43—C48—H481	119.0
C23—C24—H241	120.0	C47—C48—H481	120.0

Hydrogen-bond geometry (Å, º)

D—H···*A*	*D*—H	H···*A*	*D*···*A*	*D*—H···*A*
N27—H271···O2^{i}	0.84	2.08	2.923 (4)	176 (2)
N3—H31···O26	0.86	1.97	2.817 (4)	173 (2)

Symmetry code: (i) $x-1, y, z$.